

Periodic Curcumin Monoglucuronide Injections Ameliorate Structural Osteoarthritis Changes in Rats with Destabilized Medial Meniscus

Akihiro Nakahata

Kyoto university

Akira Ito

Kyoto university

Ryo Nakahara

Kyoto university

Atsuhiko Kishimoto

Therabiopharma Inc.

Atsushi Imaizumi

Therabiopharma Inc.

Tadashi Hashimoto

Therabiopharma inc.

Shogo Mukai

Kyoto Medical Center

Yasuaki Nakagawa

Kyoto medical Center

Hiroshi Kuroki (✉ kuroki.hiroshi.6s@kyoto-u.ac.jp)

Research article

Keywords: curcumin monoglucuronide (TBP1901), curcumin, osteoarthritis, inflammation, articular cartilage, subchondral bone, osteophyte

Posted Date: June 17th, 2020

DOI: <https://doi.org/10.21203/rs.3.rs-35501/v1>

License:   This work is licensed under a Creative Commons Attribution 4.0 International License.

[Read Full License](#)

Abstract

Background: Curcumin has anti-inflammatory effects. However, curcumin is poorly water-soluble, and when administered orally, forms curcumin conjugates with poor efficacy. Curcumin monoglucuronide (TBP1901) is highly water-soluble and can exist in the free-form in a greater proportion than curcumin in vivo. This study aimed to evaluate the effectiveness of intra-articular TBP1901 injections for a rat model of osteoarthritis (OA).

Methods: Sixty-four male Wistar rats (12 weeks old) that had received the destabilized medial meniscus (DMM) surgery, were randomly separated into the TBP1901 injection and the saline solution injection (control) group. They were sacrificed at 1, 2, 6, or 10 weeks postoperatively (n = 8 for each). The TBP1901 (30 mg/mL) and saline solution of 50 μ L were administered to the knee joint through the patella tendon twice a week for the rats sacrificed at 1 and 2 weeks or once a week for at 6 and 10 weeks. The OA changes were evaluated by micro-computed tomography (micro-CT), histology, and immunohistochemical analysis.

Results: Curcumin fluorescence was confirmed in the articular cartilage and synovium of rats with TBP1901 injections at all observation periods. The TBP1901 injections significantly reduced the synovial inflammation at 1 and 2 weeks and the expression of TNF α in the tibial articular cartilage at 6 weeks postoperatively. Moreover, TBP1901 injections ameliorated the articular cartilage structure, the subchondral bone (SB) plate thickness, and perforations from 6 to 10 weeks. As a result, there were significant differences between groups in OA scores, SB plate thickness, and perforations at 10 weeks postoperatively. In addition, osteophyte formation in the TBP1901 group was significantly suppressed after 10 weeks.

Conclusion: This study reports the first evidence that TBP1901 injections suppress inflammation and osteophyte formation, and ameliorate the articular cartilage and SB pathologies by absorption in the articular cartilage and synovium in a rat DMM model. Therefore, intra-articular injections of TBP1901 may be effective in improving OA pathology.

Introduction

Osteoarthritis (OA) is a progressive disease that affects the activity of daily living in many people worldwide. Conservative treatments for OA include physiotherapy [1, 2], dieting [3, 4], hyaluronic acid intra-articular injection [5], and non-steroidal anti-inflammatory drugs (NSAIDs) [6], and they have certain beneficial effects. However, it is difficult to prevent OA progression, while analgesic drugs such as NSAIDs have adverse effects [7, 8]. Therefore, the development of a new treatment method is needed. Curcumin, a polyphenol compound present in turmeric (*Curcuma longa*, long used as a spice and herbal medicine), has been confirmed to have many positive health benefits: anti-inflammatory [9, 10], anti-oxidative [11, 12], anti-cancer [13, 14], anti-allergy [15, 16], anti-diabetes [17], hepatoprotective [18], neuroprotective [19], anti-depressant [20], and muscle damage protective [21] effects. In a randomized control study (RCT) of

patients with knee OA, treatments with curcumin were associated with significant score reductions in the following indexes: Western Ontario and McMaster Universities Osteoarthritis Index (WOMAC), Visual Analog Scale (VAS; subjective pain scale), and Lequesne's pain functional index (LPFI) [22, 23]. Another study using a mouse OA model showed that curcumin suppressed articular cartilage destruction [24, 25]. Although beneficial effects have been confirmed, curcumin has low hydrophilicity and high lipophilicity [26]. Therefore, it is not efficiently absorbed when it is ingested [27, 28]. One of the formulations that partially solves this problem, a high absorption curcumin, increased the in vivo absorption rate 27-fold than a traditional curcumin when taken orally [29–31]. In an RCT study using a high absorption curcumin with knee OA patients, VAS scores were significantly lower in the high absorption curcumin group than in the placebo group [32].

Ingested curcumin is mostly present as molecular conjugates in the body, with almost no free-form curcumin, which is most important for pharmacological activity [33–35]. The in vitro pharmacological activity of curcumin (e.g., anticancer effects) is associated with the free-form curcumin, not curcumin monoglucuronide (TBP1901), which is the major metabolite in serum [36, 37]. The β -glucuronidase hydrolyzes TBP1901 to free curcumin [38]. It is present at high levels in tumors, and it is released from granulocytes, including neutrophils, and injured cells at sites of inflammation [39–41]. Due to this enzyme, the intravenous administration of synthesized TBP1901 in mice showed the presence of free-form curcumin in the blood at a constant level (approximately 4–16% of total curcumin levels), and the tumor growth was significantly suppressed [42]. Furthermore, the bone has been shown to contain more aglycone curcumin and curcumin than other tissues when curcumin is ingested, probably because the β -glucuronidase expressed in bone marrow cells deconjugates TBP1901 [35, 43]. Previous studies on bone diseases using curcumin have reported that the deglucuronidation activity of bone marrow cells has given bone protective effects, despite curcumin having low bioavailability [44, 45]. Therefore, TBP1901 may act as a pro-drug that targets the bone. In addition, because TBP1901 has a higher polarity than curcumin, it is more water-soluble than curcumin [42]. Its water-solubility makes it more suitable for use in injections than curcumin, and it may be also more effective for absorption into the joint tissue, which is composed mostly of water.

Taken together, these reports suggest that treatments with TBP1901 may work more effectively for the pathophysiology of the inflammatory disease OA. To verify the hypothesis, we chose the relatively slow progressing OA model of rats with destabilized medial meniscus (DMM) [46]. Thus, the purpose of this study was to investigate the effectiveness of TBP1901 in OA progression in the rat DMM model.

Methods

Animal preparation and surgical procedures

This study was approved by the animal research committee of Kyoto University (approval number: Med Kyo 19016) and conducted in accordance with the ARRIVE guidelines [47].

Sixty-four male Wistar rats (12 weeks old), purchased from SHIMIZU Laboratory Supplies Co. Ltd. (Kyoto, Japan), were placed in a plastic cage with paper bedding on a 12-h light/dark cycle at a constant temperature. The rats could move freely in the cages and had free access to food and water. All rats underwent DMM surgery for the OA model [46]. Briefly, DMM surgery was performed with anteromedial capsule incision and transection of the medial meniscotibial ligament in the right knee under anesthesia with 1.0 mL/kg pentobarbital sodium (Somnopenyl; Kyoritsu Seiyaku Corp., Tokyo, Japan). The rats were randomly separated into TBP1901 and saline solution (control) injection groups (n = 32 for each group). They were sacrificed at four periods of 1, 2, 6, or 10 weeks postoperatively (n = 8 for each). The synthesis of TBP1901 was performed as described previously [42]. TBP1901 and saline injections of 50 μ L were administered to the right knee joints through the patellar tendon. The concentration of TBP1901 was chosen to be 30 mg/mL based on a preliminary study. The rats sacrificed at 1 week postoperatively were injected at day-3 and day-7 postoperatively, and at 2 weeks were injected at day-3, day-7, day-10, and day-14, and at 6 and 10 weeks were injected once a week from 1 week postoperatively. An hour after the final injection in each observation period, the rats were sacrificed by a lethal dose of pentobarbital sodium, and their right knee joints were harvested for micro-computed tomography (micro-CT), histochemical, and immunohistochemical analysis. Bodyweight was measured every week for all rats.

Micro-CT analysis

After fixation of the knees with 4% paraformaldehyde overnight, the tibiofemoral (TF) joints were scanned using a micro-CT system (SMX-100CT, Shimadzu, Kyoto, Japan) at 43 kV and 43 μ A with a scan time of approximately 10 minutes. After scanning, the three-dimensional (3D) reconstruction and assessment of the TF joint were performed with ImageJ (National Institutes of Health, Bethesda, MD, USA) and Amira® (version 5.5, EFI Visualization Science Group, Burlington, MA, USA) software. The subchondral bone (SB) plate thickness, number of SB plate perforations, diameter of SB plate perforations, bone volume (BV), total volume (TV), and osteophyte volume in the medial tibia SB (above epiphyseal plate) were calculated according to protocols described in previous studies [48, 49]. SB plate thickness was measured at the thickest region around the center of the medial articular surface. The diameter of the SB plate perforation was defined as the largest diameter of the largest perforation in each sample. To assess the bone density of the SB, bone volume was divided by total volume (BV/TV).

Histological analysis

After micro-CT, the knee joint samples were decalcified in 10% ethylene-diamine-tetra-acetic acid (EDTA) for three to four weeks and cut along the mid-sagittal plane at the halfway point. After decalcification, the samples were paraffin-embedded and cut into 6 μ m sections at 50 μ m intervals. First, the paraffin sections were observed with an epifluorescence microscope (MVX10, Olympus Corporation, Tokyo, Japan) to confirm the presence of curcumin in the articular cartilage and the synovium. Curcumin is a fluorescent substance with an excitation wavelength of 300–550 nm (maximum excitation wavelength: 467 nm) and an emission wavelength of 548–600 nm (maximum emission wavelength: 571 nm) [50]. Fluorescence detection was used for curcumin quantification [51]. Based on this report, curcumin

fluorescence was observed with the mirror unit of U-MYFPHQ/XL (Olympus Corporation, Tokyo, Japan). Second, the paraffin sections were stained with hematoxylin and eosin (H/E) to evaluate the inflammation of the synovium in knee joints and Safranin O/Fast green to evaluate the severity of the cartilage degeneration and the SB changes. Inflammation was assessed using an inflammation scoring system described in a previous study [52]. Three membrane features (synovial lining cell layer, stroma cell density, and inflammatory infiltrate) were assessed in the whole knee joint as 0 (none), 1 (slight), 2 (moderate), or 3 (strong). The inflammation score was determined as the summed score for all parameters. The highest inflammation score was recorded for each sample. Cartilage degeneration was assessed using the OARSI score [53] and the modified Mankin (MM) score [54], according to a previous study. The OARSI score consists of six grades and four stages on a scale from 0 (intact) to 24 (severe damage). The MM score consists of three features (pericellular matrix staining, spatial arrangement of chondrocytes, and inter-territorial matrix staining) on a scale from 0 (intact) to 8 (severe). Cartilage degeneration was evaluated on the medial TF joint and patellofemoral (PF) joint. The maximum score was used for all scoring systems and samples.

Immunohistochemical analysis

Immunohistochemistry of type I collagen, type II collagen, Interleukin-1 β (IL1 β), Interleukin-6 (IL6), and tumor necrosis factor- α (TNF α) was performed to determine the principal collagen expression and inflammation in the cartilage. Antigen retrieval was performed for 20 minutes by heating with HistoVT One (Nacalai Tesque, Inc., Kyoto, Japan). Blocking was performed using 0.3% H₂O₂ for 15 minutes and 5% goat serum for 20 minutes at room temperature. The sections were then incubated at 4 °C overnight with primary antibodies against type I collagen (AB755P, diluted 1:1000; Merck KGaA, Darmstadt, Germany), type II collagen (diluted 1:100; KYOWA PHARMA CHEMICAL CO., LTD., Toyama, Japan), IL1 β (ab9722, diluted 1:100; Abcam Co., Cambridge, UK), IL6 (ab9324, diluted 1:250; Abcam Co., Cambridge, UK), and TNF α (ab6671, diluted 1:100; Abcam Co., Cambridge, UK). Detection was performed using the streptavidin-biotin-peroxidase complex technique with an Elite ABC kit (Vector Laboratories, CA, USA), and immunoreactivity was visualized by incubation with a diaminobenzidine solution (Vector Laboratories, CA, USA) followed by counterstaining with hematoxylin. The primary antibody was omitted from the negative control slides. The expression of type I and type II collagen in the medial tibia and patella cartilage was analyzed by measuring the minimum and mean pixel intensity values using TIFF images (magnification \times 40) taken by microscopy and ImageJ, respectively, on a scale of 0 (maximum staining) to 255 (no staining), according to a previous study [55]. The expression of IL1 β , IL6, and TNF α in the medial tibia and patella cartilage was analyzed by measuring the percentage of positive chondrocytes to detect the severity of cartilage inflammation within the middle region of the medial tibia with an anteroposterior width of 0.5 mm or the central region of the patella with a superoinferior width of 0.5 mm.

Statistical analyses

The median and interquartile range (IQR) of the inflammation score, OARSI score, and MM score (non-parametric data) were calculated for each group, and the Wilcoxon test was used to compare differences

between the two groups. In addition, the mean and 95% confidence intervals (CIs) of body weight, immunohistochemical, and micro-CT analysis data (parametric data) were calculated, and Welch's T-test was used to compare differences between the groups. The normality of the data was assessed using normal quantile–quantile plots and the Shapiro-Wilk test. P-values < 0.05 were considered statistically significant in all tests. Statistical analyses were performed with JMP® Pro 14 software (SAS Institute Inc., Cary, NC, USA).

Results

Bodyweight is shown in Supplemental Fig. 1. Bodyweight in the TBP1901 group was significantly lower than that in the control group at 1 week (mean (95% CIs): 276.59 g (272.65–280.54); TBP1901, 282.31 g (278.40–286.23); control, $p = 0.04$), but after 1 week, there were no significant differences between groups. There were no other adverse events.

Histology

Curcumin fluorescence was confirmed in the tibial articular cartilage at all observation periods in rats with TBP1901 injections (Fig. 1), although it was very weak at 10 weeks. The fluorescence was most strongly expressed at 2 weeks. In the synovium, curcumin fluorescence was confirmed at all observation periods in rats with TBP1901 injections. The fluorescence was strongly expressed 2 weeks after synovial growth. In addition, fluorescence expression was confirmed in control sections at 2 weeks. There was a difference in the strongly positive periods of fluorescence expression between the articular cartilage and the synovium.

Severe synovial inflammation was especially observed at 1 and 2 weeks postoperatively as an enlargement of the synovial lining cell layer and increased cellularity and situated lymphocytes or plasma cells (Fig. 2). The TBP1901 injections significantly reduced the synovial inflammation at 1 ($p = 0.007$) and 2 weeks ($p < 0.001$) postoperatively. However, no significant effects were seen after 6 weeks when the inflammation had subsided.

Articular cartilage damage of the medial tibia tended to worsen over time in the controls. However, in the TBP1901 group, the articular cartilage structure ameliorated from 6 to 10 weeks (Fig. 3A). The cartilage structure was preserved in most subjects of the TBP1901 group at 10 weeks. The OARSI and MM scores in the TBP1901 group were significantly lower than the scores in the control group at 10 weeks ($p < 0.001$, each).

On the contrary, the articular cartilage of the patella displayed some damage from 1 to 10 weeks (Fig. 3B). However, the cartilage structure of the patella also ameliorated from 6 to 10 weeks in the TBP1901 group. At 10 weeks, TBP1901 injections reduced the fibrillation of the cartilage surface. The OARSI score in the TBP1901 group was significantly lower than that in the control group at 10 weeks ($p = 0.003$). The TBP1901 prevented the reduction of SafraninO staining at 1 week. The MM score in the TBP1901 group was significantly lower than that in the control group at 1 week ($p = 0.025$).

Immunohistochemistry

Tibiofemoral joint

The expression of type I collagen was confirmed on the surface of the articular cartilage in the medial tibia in all observation periods. There were no differences between the groups (Fig. 4A). The abnormal expression of type II collagen in the articular cartilage was confirmed at 1 and 2 weeks postoperatively. At 1, 2, and 6 weeks, there were no significant differences in mean intensity between the groups. However, TBP1901 injections significantly increased the expression at 10 weeks.

The pro-inflammatory cytokine expression levels of IL1 β , IL6, and TNF α were confirmed in the articular cartilage of the tibia (Fig. 5). The percentages of positive chondrocytes increased from 1 week to 10 weeks. There were no significant differences between groups at weeks 1, 2, and 10, but TBP1901 injections significantly reduced TNF α expression at 6 weeks ($p = 0.02$). In addition, TBP1901 injections showed a tendency to reduce IL6 expression at 6 weeks.

Patellofemoral joint

The expression of type I collagen was almost undetectable in the patellar articular cartilage at 1, 2, and 6 weeks and was confirmed at 10 weeks on the surface of the cartilage (Fig. 4B). There were no significant differences between the groups. The expression of type II collagen in the patella was stable, unlike that in the tibia. There were few differences among the observation periods, but TBP1901 injections significantly increased the type II collagen expression at 10 weeks ($p = 0.016$).

The pro-inflammatory cytokines IL1 β , IL6, and TNF α were more highly expressed in the articular cartilage of the patella than in the tibia (Fig. 6). The percentage of positive chondrocytes slightly decreased from 1 week to 10 weeks. There were no significant differences between groups at 1, 2, and 10 weeks, but TBP1901 injections significantly increased IL6 and IL1 β expression at 6 weeks ($p = 0.001$ each). However, the TNF α expression in the TBP1901 group showed a tendency to decrease at 6 weeks.

Micro-CT analysis

The DMM surgery induced SB changes and osteophyte formation (Fig. 7A & 7B). In the control group, the SB plate thickness decreased from 1 week to 2 weeks and increased after 2 weeks (Fig. 7B). However, in the TBP1901 group, the SB plate thickness did not decrease from 1 week to 2 weeks. After that, it became thicker by week 6 and decreased by week 10. There were significant differences in SB plate thickness at 2 ($p = 0.002$), 6 ($p = 0.029$), and 10 weeks ($p = 0.002$) between groups. In particular, TBP1901 injections reduced the thickness in 10 weeks compared with the control group.

SB plate perforations were found by micro-CT images especially after 6 weeks (Fig. 7A). There were no differences in the number and diameter of SB plate perforations at 6 weeks between the groups, but TBP1901 injections significantly reduced them in 10 weeks compared with the control group ($p < 0.001$ and $p = 0.001$, respectively; Fig. 7B).

The BV/TV in the SB of the medial tibia tended to increase from 1 week to 10 weeks (Fig. 7B). The TBP1901 injections significantly decreased BV/TV in 2 weeks ($p = 0.013$). However, the BV/TV in the TBP1901 group was significantly larger at 6 weeks ($p = 0.004$). There was no significant difference at 10 weeks between the groups.

The osteophytes on the medial tibia had formed 2 weeks postoperatively. The osteophyte volume in the TBP1901 group tended to be lower than that in the control group at 6 weeks, and TBP1901 injections significantly suppressed osteophyte growth at 10 weeks compared with the control group ($p < 0.001$).

Discussion

In this study, we performed intra-articular injections of TBP1901, a curcumin prodrug, at 1, 2, 6, or 10 weeks after the DMM operation to examine whether it prevented OA progression in rat knees. Curcumin fluorescence was confirmed in the articular cartilage and synovium in the TBP1901 group. The TBP1901 injections suppressed TNF α expression in 6 weeks and ameliorated the articular cartilage structure in 10 weeks. The TBP1901 reduced SB plate thickness and perforations in 10 weeks. This study revealed that TBP1901 injections have a preventive or ameliorative effect on OA progression in this study.

Curcumin fluorescence after TBP1901 injection

Curcumin fluorescence was confirmed in the articular cartilage and synovium after TBP1901 injections. It is known that autofluorescence appears more pronounced in inflamed tissues or synovium [56, 57]. We also measured some autofluorescence from the inflamed synovial cells and tissue in our study, as positive fluorescence was found in the synovium of controls at 2 and 6 weeks. However, the differences between groups were obvious to us, and we feel this must reflect curcumin fluorescence. This is the first report to confirm curcumin fluorescence after TBP1901 injections, to our knowledge. It is hypothesized that while TBP1901 entered each tissue, it was hydrolyzed to free aglycons by glucuronidase in the tissues or that it entered each tissue after hydrolyzation. There are no reports in the literature that suggest that administered curcumin is absorbed by articular cartilage; therefore, a highly water-soluble TBP1901 may be more suitable for absorption into articular cartilage.

In addition, curcumin fluorescence was observed at 6 weeks postoperatively, suggesting that hydrolysis of TBP1901 can occur even during the non-hyperacute phase. Furthermore, the timing of curcumin fluorescence expression in the articular cartilage and synovium was different; thus, the timing of administration may need to be considered depending on the expected effect.

Anti-inflammatory effect and articular cartilage ameliorated by TBP1901

This is the first report to show the effect of anti-inflammation and anti-OA progression by TBP1901 injections in rat knee joints. Inflammation plays a central role in OA pathogenesis. Inflammation contributes to chondrocyte apoptosis, extracellular matrix disruption, and cartilage degeneration through the pro-inflammatory cytokines IL1 β , IL6, and TNF- α [58–64]. Curcumin has been suggested to suppress

inflammation and prevent cartilage destruction by reducing the activation of the NF- κ B pathway and pro-inflammatory cytokine expression [25, 65–67].

In our study, TBP1901 injections reduced the pro-inflammatory cytokine expression in articular cartilage in 6 weeks and ameliorated the articular cartilage structure in 10 weeks. No previous studies using curcumin have shown the restoration of cartilage structure to our knowledge, but in our hands, TBP1901 injections ameliorated the cartilage damage from 6 weeks to 10 weeks. Besides, curcumin promotes chondrogenic differentiation of mesenchymal stem cells (MSCs) [68], and has the potential to promote self-healing of articular cartilage. Our results suggest that the curcumin in the joint, may maximize the self-healing effect of curcumin with anti-inflammation. On the other hand, in the early period after DMM surgery, 1, 2, and 6 weeks postoperatively, there were no significant differences in the TF articular cartilage between the two groups. The reason for this might have been a more rapid OA progression, even though DMM surgery normally induces OA changes relatively slowly in the OA model.

Effect of TBP1901 on subchondral bone

Moreover, this study showed the beneficial effects on SB and osteophyte formation. Few reports have shown that curcumin is effective for SB. Zhang et al. reported that oral administration of curcumin for 8 weeks reduced SB plate thickness [25]. In our study, TBP1901 injections in 10 weeks suppressed SB plate thickening. A similar tendency was observed with the degree of articular cartilage status, so that the articular cartilage and SB may have been interrelated.

Generally, the SB plate becomes thinner due to increased bone remodeling in early OA and thicker due to changes in remodeling balance as OA progresses [69, 70]. However, TBP1901 suppressed SB plate thinning in 2 weeks. Some reports have shown that curcumin attenuates bone resorption by suppressing osteoclast proliferation [71] and osteoblast apoptosis [72]. This may be one of the reasons why the SB plate thinning was suppressed by TBP1901. Moreover, mechanical loading changes related to pain relief may have affected SB plate thickness because curcumin has a pain relief effect [25, 32]. In addition, TBP1901 reduced SB plate perforations in 10 weeks, indicating that TBP1901 could affect bone reformation in the SB.

Moreover, TBP1901 injections suppressed osteophyte formation. Osteophytes are a representative pathophysiology of OA and cause limitations in range of motion. Osteophytes are formed by cells (e.g., MSCs) in the synovium in a process similar to endochondral ossification [73]. In osteophyte formation, transforming growth factor- β (TGF β) and macrophages play an important role [74, 75]. In addition, oral curcumin administration induced the suppression of TGF β activation on the synovium in a previous report [76]. In our study, curcumin fluorescence was confirmed in the synovium at even 10 weeks postoperatively, so that suppression of TGF β activation by curcumin might suppress osteophyte formation. This study indicated that TBP1901 has significant beneficial effects on the SB and osteophytes, which were less seen in previous reports of administered curcumin. These remarkable effects for SB and osteophytes may be due to the presence of free curcumin derived from TBP1901 hydrolyzed by one of the many glucuronidases produced in the bone marrow [35, 42].

Limitations And Conclusion

The present study has some limitations. First, it has not been determined whether TBP1901 is more effective than curcumin or a high absorption curcumin, since no comparative studies have been conducted. A comparative study is needed to reveal this. Second, although the DMM model exhibits similar histological features to human OA, the model shows more rapid progression than typical human OA [77,78]. An experiment using a slower OA progression model is needed to reveal its effect on early OA. Third, it is insufficient to conclude whether TBP1901 induces reversible cartilage restoration from this study. It would be necessary to follow-up the same individual or conduct an experiment to administer TBP1901 after articular cartilage damage. Fourth, it is unclear how and where TBP1901 was hydrolyzed to curcumin in the joint, although curcumin fluorescence was confirmed in the articular cartilage. Moreover, the excitation and emission wavelengths of curcumin conjugates are unclear, so the curcumin fluorescence in this study may include fluorescence from curcumin conjugates. Fifth, the mechanism of the effect of TBP1901 on SB and osteophyte formation is unclear. Additional comprehensive studies focusing on TGF β , macrophages, and mechanical stress are necessary. Sixth, it is unclear what dosage would be best to administer TBP1901, although it was administered at 30mg/mL by intra-articular injections from the hyperacute phase in this study. Additional investigations are necessary to determine the best postoperative timing and mode of administration of TBP1901.

In conclusion, this study showed the first evidence of curcumin fluorescence in articular cartilage and synovium following intra-articular injections of TBP1901. Furthermore, its injections ameliorated the articular cartilage structure and SB homeostasis in a rat OA model (DMM), following the reduction of synovial inflammation and TNF α expression (Fig. 8). Moreover, no adverse events other than a slight decrease in weight gain were observed at the beginning of injections. Similar effects may be expected for human trials, but additional experiments are required.

Abbreviations:

TBP1901, curcumin monoglucuronide; OA, osteoarthritis; DMM, destabilized medial meniscus; SB, subchondral bone; CT, computed tomography; RCT, randomized control study; WOMAC, Western Ontario and McMaster Universities Osteoarthritis Index; VAS, Visual Analog Scale; LPFI, Lequesne's pain functional index; TF joint, tibiofemoral joint; 3D, three-dimensional; BV, bone volume; TV, total volume; EDTA, ethylenediaminetetraacetic acid; H/E, Hematoxylin/Eosin; MM score, modified mankin score; PF joint, patellofemoral joint; IL1 β , Interleukin-1 β ; IL6, Interleukin-6; TNF α , Tumor Necrosis Factor- α ; IQR, interquartile range; CIs, confidence intervals; MSCs, Mesenchymal Stem Cells; TGF β , Transforming growth factor- β

Declarations

Ethics approval and consent to participate

Not applicable

Consent for publication

Not applicable

Availability of data and materials

The datasets used and/or analyzed during the current study are available from the corresponding author upon reasonable request.

Competing interests

This study was funded by Therabiopharma Inc. Atl and TH have equity in Therabiopharma Inc. and serve on the board of directors of Therabiopharma Inc. AK is an employee of Therabiopharma Inc.

Funding

This study was supported in part by JSPS KAKENHI Grant Numbers JP18H03129 and JP18K19739, and a sponsored research grant from Therabiopharma Inc. to HK.

Author contributions

AN contributed to the conception and design of the study; the acquisition, analysis, and interpretation of the data; and drafted the article. AK contributed to the conception and design of the study, interpretation of the data, and revision of the manuscript. RN contributed to animal surgery and revision of the manuscript. AK contributed to producing the TBP1901 and revising the manuscript. Atl contributed to the conception and design of the study, producing the TBP1901, and revising the manuscript. TH, SM and YN contributed to the conception and design of the study and revision of the manuscript. HK contributed to the conception and design of the study, interpretation of the data, and revision of the manuscript. All authors have read and approved the final manuscript.

Acknowledgements

We would like to thank Editage (www.editage.com) for English language editing.

References

1. Yamato TP, Deveza LA, Maher CG. Exercise for osteoarthritis of the knee (PEDro synthesis). *Br J Sports Med*. 2016;50(16):1013–4.
2. Verhagen AP, Ferreira M, Reijnen-van de Vendel EAE, Teirlinck CH, Runhaar J, van Middelkoop M, et al. Do we need another trial on exercise in patients with knee osteoarthritis?: No new trials on exercise in knee OA. *Osteoarthr Cartil [Internet]*. 2019;27(9):1266–9. <https://doi.org/10.1016/j.joca.2019.04.020>.

3. Messier SP, Mihalko SL, Legault C, Miller GD, Nicklas BJ, DeVita P, et al. Effects of intensive diet and exercise on knee joint loads, inflammation, and clinical outcomes among overweight and obese adults with knee osteoarthritis: The IDEA randomized clinical trial. *JAMA - J Am Med Assoc*. 2013;310(12):1263–73.
4. Hall M, Castelein B, Wittoek R, Calders P, Van Ginckel A. Diet-induced weight loss alone or combined with exercise in overweight or obese people with knee osteoarthritis: A systematic review and meta-analysis. *Semin Arthritis Rheum* [Internet]. 2019;48(5):765–77. <https://doi.org/10.1016/j.semarthrit.2018.06.005>.
5. Concoff A, Sancheti P, Niazi F, Shaw P, Rosen J. The efficacy of multiple versus single hyaluronic acid injections: A systematic review and meta-analysis. *BMC Musculoskelet Disord*. 2017;18(1):1–14.
6. McAlindon TE, Bannuru RR, Sullivan MC, Arden NK, Berenbaum F, Bierma-Zeinstra SM, et al. OARSI guidelines for the non-surgical management of knee osteoarthritis. *Osteoarthr Cartil* [Internet]. 2014;22(3):363–88. <http://dx.doi.org/10.1016/j.joca.2014.01.003>.
7. Baigent C, Bhala N, Emberson J, Merhi A, Abramson S, Arber N, et al. Vascular and upper gastrointestinal effects of non-steroidal anti-inflammatory drugs: Meta-analyses of individual participant data from randomised trials. *Lancet* [Internet]. 2013;382(9894):769–79. [http://dx.doi.org/10.1016/S0140-6736\(13\)60900-9](http://dx.doi.org/10.1016/S0140-6736(13)60900-9).
8. Cooper C, Chapurlat R, Al-Daghri N, Herrero-Beaumont G, Bruyère O, Rannou F, et al. Safety of Oral Non-Selective Non-Steroidal Anti-Inflammatory Drugs in Osteoarthritis: What Does the Literature Say? *Drugs Aging* [Internet]. 2019;36(s1):15–24. <https://doi.org/10.1007/s40266-019-00660-1>.
9. Srimal RC, Dhawan BN. Pharmacology of diferuloyl methane (curcumin), a non-steroidal anti-inflammatory agent. *J Pharm Pharmacol*. 1973;25(6):447–52.
10. Jurenka JS. Anti-inflammatory properties of curcumin, a major constituent of *Curcuma longa*: A review of preclinical and clinical research. *Altern Med Rev*. 2009;14(2):141–53.
11. Sugiyama Y, Kawakishi S, Osawa T. Involvement of the β -diketone moiety in the antioxidative mechanism of tetrahydrocurcumin. *Biochem Pharmacol*. 1996;52(4):519–25.
12. Wright JS. Predicting the antioxidant activity of curcumin and curcuminoids. *J Mol Struct THEOCHEM*. 2002;591(1–3):207–17.
13. Aggarwal BB, Kumar A, Bharti AC. Anticancer potential of curcumin: Preclinical and clinical studies. *Anticancer Res*. 2003;23(1 A):363–98.
14. Patel BB, Gupta D, Elliott AA, Sengupta V, Yu YMA. Curcumin Targets FOLFOX-surviving Colon Cancer Cells via Inhibition of EGFRs and IGF-1R. *Anticancer Res*. 2010;30(2):319–25.
15. Ram A, Das M, Ghosh B. Curcumin attenuates allergen-induced airway hyperresponsiveness in sensitized guinea pigs. *Biol Pharm Bull*. 2003;26(7):1021–4.
16. Kurup VP, Barrios CS, Raju R, Johnson BD, Levy MB, Fink JN. Immune response modulation by curcumin in a latex allergy model. *Clin Mol Allergy*. 2007;5:1–12.
17. Mahesh T, Sri Balasubashini MM, Menon VP. Photo-irradiated curcumin supplementation in streptozotocin-induced diabetic rats: Effect on lipid peroxidation. Vol. 59, *Therapie*. 2004. p. 639–44.

18. Nabavi SF, Daglia M, Moghaddam AH, Habtemariam S, Nabavi SM. Curcumin and liver disease: From chemistry to medicine. *Compr Rev Food Sci Food Saf*. 2014;13(1):62–77.
19. Yang F, Lim GP, Begum AN, Ubeda OJ, Simmons MR, Ambegaokar SS, et al. Curcumin inhibits formation of amyloid β oligomers and fibrils, binds plaques, and reduces amyloid in vivo. *J Biol Chem*. 2005;280(7):5892–901.
20. Kulkarni SK, Bhutani MK, Bishnoi M. Antidepressant activity of curcumin: Involvement of serotonin and dopamine system. *Psychopharmacology*. 2008;201(3):435–42.
21. Davis JM, Murphy EA, Carmichael MD, Zielinski MR, Groschwitz CM, Brown AS, et al. Curcumin effects on inflammation and performance recovery following eccentric exercise-induced muscle damage. *Am J Physiol - Regul Integr Comp Physiol*. 2007;292(6):2168–73.
22. Panahi Y, Rahimnia AR, Sharafi M, Alishiri G, Saburi A, Sahebkar A. Curcuminoid treatment for knee osteoarthritis: A randomized double-blind placebo-controlled trial. *Phyther Res*. 2014;28(11):1625–31.
23. Daily JW, Yang M, Park S. Efficacy of Turmeric Extracts and Curcumin for Alleviating the Symptoms of Joint Arthritis: A Systematic Review and Meta-Analysis of Randomized Clinical Trials. *J Med Food*. 2016;19(8):717–29.
24. Zhang G, Cao J, Yang E, Liang B, Ding J, Liang J, et al. Curcumin improves age-related and surgically induced osteoarthritis by promoting autophagy in mice. *Biosci Rep [Internet]*. 2018;38(4):BSR20171691. <http://bioscirep.org/lookup/doi/10.1042/BSR20171691>.
25. Zhang Z, Leong DJ, Xu L, He Z, Wang A, Navati M, et al. Curcumin slows osteoarthritis progression and relieves osteoarthritis-associated pain symptoms in a post-traumatic osteoarthritis mouse model. *Arthritis Res Ther [Internet]*. 2016;18(1):1–12. <http://dx.doi.org/10.1186/s13075-016-1025-y>.
26. Tønnesen HH. Solubility and stability of curcumin in solutions containing alginate and other viscosity modifying macromolecules: Studies of curcumin and curcuminoids. *XXX Pharmazie*. 2006;61(8):696–700.
27. Yang KY, Lin LC, Tseng TY, Wang SC, Tsai TH. Oral bioavailability of curcumin in rat and the herbal analysis from *Curcuma longa* by LC-MS/MS. *J Chromatogr B Anal Technol Biomed Life Sci*. 2007;853(1–2):183–9.
28. Lao CD, Ruffin IVMT, Normolle D, Heath DD, Murray SI, Bailey JM, et al. Dose escalation of a curcuminoid formulation. *BMC Complement Altern Med*. 2006;6:4–7.
29. Sunagawa Y, Hirano S, Katanasaka Y, Miyazaki Y, Funamoto M, Okamura N, et al. Colloidal submicron-particle curcumin exhibits high absorption efficiency—a double-blind, 3-way crossover study. *J Nutr Sci Vitaminol (Tokyo)*. 2015;61(1):37–44.
30. Morimoto T, Sunagawa Y, Katanasaka Y, Hirano S, Namiki M, Watanabe Y, et al. Drinkable preparation of theracurmin exhibits high absorption efficiency—a single-dose, double-blind, 4-way crossover study. *Biol Pharm Bull*. 2013;36(11):1708–14.
31. Sasaki H, Sunagawa Y, Takahashi K, Imaizumi A, Fukuda H, Hashimoto T, et al. Innovative preparation of curcumin for improved oral bioavailability. *Biol Pharm Bull*. 2011;34(5):660–5.

32. Nakagawa Y, Mukai S, Yamada S, Matsuoka M, Tarumi E, Hashimoto T, et al. Short-term effects of highly-bioavailable curcumin for treating knee osteoarthritis: a randomized, double-blind, placebo-controlled prospective study. *J Orthop Sci [Internet]*. 2014;19(6):933–9. <http://dx.doi.org/10.1007/s00776-014-0633-0>.
33. Vareed SK, Kakarala M, Ruffin MT, Crowell JA, Normolle DP, Djuric Z, et al. Pharmacokinetics of curcumin conjugate metabolites in healthy human subjects. *Cancer Epidemiol Biomarkers Prev*. 2008;17(6):1411–7.
34. Pan MH, Huang TM, Lin JK. Biotransformation of curcumin through reduction and glucuronidation in mice. *Drug Metab Dispos*. 1999;27(4):486–94.
35. Kunihiro AG, Brickey JA, Frye JB, Luis PB, Schneider C, Funk JL. Curcumin, but not curcumin-glucuronide, inhibits Smad signaling in TGF β -dependent bone metastatic breast cancer cells and is enriched in bone compared to other tissues. *J Nutr Biochem [Internet]*. 2019;63:150–6. <https://doi.org/10.1016/j.jnutbio.2018.09.021>.
36. Shoji M, Nakagawa K, Watanabe A, Tsuduki T, Yamada T, Kuwahara S, et al. Comparison of the effects of curcumin and curcumin glucuronide in human hepatocellular carcinoma HepG2 cells. *Food Chem [Internet]*. 2014;151:126–32. <http://dx.doi.org/10.1016/j.foodchem.2013.11.021>.
37. Pal A, Sung B, Bhanu Prasad BA, Schuber PT, Prasad S, Aggarwal BB, et al. Curcumin glucuronides: Assessing the proliferative activity against human cell lines. *Bioorganic Med Chem [Internet]*. 2014;22(1):435–9. <http://dx.doi.org/10.1016/j.bmc.2013.11.006>.
38. Sperker B, Backman JT, Kroemer HK. The role of β -glucuronidase in drug disposition and drug targeting in humans. *Clin Pharmacokinet*. 1997;33(1):18–31.
39. Mürdter TE, Sperker B, Kivistö KT, McClellan M, Fritz P, Friedel G, et al. Enhanced uptake of doxorubicin into bronchial carcinoma: β -glucuronidase mediates release of doxorubicin from a glucuronide prodrug (HMR 1826) at the tumor site. *Cancer Res*. 1997;57(12):2440–5.
40. Marshall T, Shult P, Busse WW. Release of lysosomal enzyme beta-glucuronidase from isolated human eosinophils. *J Allergy Clin Immunol*. 1988;82(4):550–5.
41. Shimoi K, Nakayama T. Glucuronidase deconjugation in inflammation. *Methods Enzymol*. 2005;400(1994):263–72.
42. Ozawa H, Imaizumi A, Sumi Y, Hashimoto T, Kanai M, Makino Y, et al. Curcumin β -D-glucuronide plays an important role to keep high levels of free-form curcumin in the blood. *Biol Pharm Bull*. 2017;40(9):1515–24.
43. Kunihiro AG, Luis PB, Brickey JA, Frye JB, Chow HHS, Schneider C, et al. Beta-Glucuronidase Catalyzes Deconjugation and Activation of Curcumin-Glucuronide in Bone. *J Nat Prod*. 2019;82(3):500–9.
44. French DL, Muir JM, Webber CE. The ovariectomized, mature rat model of postmenopausal osteoporosis: An assessment of the bone sparing effects of curcumin. *Phytomedicine*. 2008;15(12):1069–78.

45. Funk JL, Frye JB, Oyarzo JN, Kuscuoglu N, Wilson J, McCaffrey G, et al. Efficacy and mechanism of action of turmeric supplements in the treatment of experimental arthritis. *Arthritis Rheum.* 2006;54(11):3452–64.
46. Glasson SS, Blanchet TJ, Morris EA. The surgical destabilization of the medial meniscus (DMM) model of osteoarthritis in the 129 / SvEv mouse. 2007;1061–9.
47. Kilkenny C, Browne WJ, Cuthill IC, Emerson M, Altman DG. Improving bioscience research reporting: The arrive guidelines for reporting animal research. *PLoS Biol.* 2010;8(6):6–10.
48. Iijima H, Aoyama T, Ito A, Tajino J, Yamaguchi S, Nagai M, et al. Exercise intervention increases expression of bone morphogenetic proteins and prevents the progression of cartilage-subchondral bone lesions in a post-traumatic rat knee model. *Osteoarthr Cartil [Internet]*. 2016;24(6):1092–102. <http://dx.doi.org/10.1016/j.joca.2016.01.006>.
49. Iijima H, Ito A, Nagai M, Tajino J, Yamaguchi S, Kiyaw W, et al. Physiological exercise loading suppresses post-traumatic osteoarthritis progression via an increase in bone morphogenetic proteins expression in an experimental rat knee model. *Osteoarthr Cartil [Internet]*. 2017;25(6):964–75. <http://dx.doi.org/10.1016/j.joca.2016.12.008>.
50. Ali Z, Saleem M, Atta BM, Khan SS, Hammad G. Determination of curcuminoid content in turmeric using fluorescence spectroscopy. *Spectrochim Acta - Part A Mol Biomol Spectrosc.* 2019;213:192–8.
51. Jasim F, Ali F. A novel and rapid method for the spectrofluorometric determination of curcumin in curcumin spices and flavors. *Microchem J.* 1992;46(2):209–14.
52. Krenn V, Morawietz L, Burmester GR, Kinne RW, Mueller-Ladner U, Muller B, et al. Synovitis score: Discrimination between chronic low-grade and high-grade synovitis. *Histopathology.* 2006;49(4):358–64.
53. Pritzker KPHMD, C FRCP, Gay SMD, Jimenez SAMD, Ostergaard KMD, Ph D, et al. Osteoarthritis cartilage histopathology: grading and staging 1, 2. 2006.
54. Bomsta BD, Bridgewater LC, Seegmiller RE. Premature osteoarthritis in the Disproportionate micromelia (Dmm) mouse. *Osteoarthr Cartil.* 2006;14(5):477–85.
55. Iijima H, Aoyama T, Ito A, Tajino J, Nagai M, Zhang X, et al. Immature articular cartilage and subchondral bone covered by menisci are potentially susceptible to mechanical load. *BMC Musculoskelet Disord [Internet]*. 2014;15(1):1–12.
56. Wizenty J, Ashraf MI, Rohwer N, Stockmann M, Weiss S, Biebl M, et al. Autofluorescence: A potential pitfall in immunofluorescence-based inflammation grading. *J Immunol Methods.* 2018;456(February):28–37.
57. Eerola E, Pulkki K, Pelliniemi LJ, Granfors K, Vuorio E, Toivanen A. Arthritis-associated changes in flow cytometric characteristics of cultured synovial fibroblasts. *Arthritis Rheum.* 1988;31(3):339–47.
58. Lieberthal J, Sambamurthy N, Scanzello CR. Inflammation in joint injury and post-traumatic osteoarthritis. *Osteoarthr Cartil [Internet]*. 2015;23(11):1825–34. <http://dx.doi.org/10.1016/j.joca.2015.08.015>.

59. Huebner KD, Shrive NG, Frank CB. New surgical model of post-traumatic osteoarthritis: Isolated intra-articular bone injury in the rabbit. *J Orthop Res*. 2013;31(6):914–20.
60. Heard BJ, Solbak NM, Achari Y, Chung M, Hart DA, Shrive NG, et al. Changes of early post-traumatic osteoarthritis in an ovine model of simulated ACL reconstruction are associated with transient acute post-injury synovial inflammation and tissue catabolism. *Osteoarthr Cartil* [Internet]. 2013;21(12):1942–9. <http://dx.doi.org/10.1016/j.joca.2013.08.019>.
61. Glasson S. In Vivo Osteoarthritis Target Validation Utilizing Genetically-Modified Mice. *Curr Drug Targets*. 2007;Vol. 8:367–76.
62. Kapoor M, Martel-Pelletier J, Lajeunesse D, Pelletier JP, Fahmi H. Role of proinflammatory cytokines in the pathophysiology of osteoarthritis. *Nat Rev Rheumatol*. 2011;7(1):33–42.
63. Jia PT, Zhang XL, Zuo HN, Lu X, Li L. Articular cartilage degradation is prevented by tanshinone IIA through inhibiting apoptosis and the expression of inflammatory cytokines. *Mol Med Rep*. 2017;16(5):6285–9.
64. Aizawa T, Kon T, Einhorn TA, Gerstenfeld LC. Induction of apoptosis in chondrocytes by tumor necrosis factor-alpha. *J Orthop Res*. 2001;19(5):785–96.
65. Yan D, He B, Guo J, Li S, Wang J. Involvement of TLR4 in the protective effect of intra-articular administration of curcumin on rat experimental osteoarthritis. *Acta Cir Bras*. 2019;34(6).
66. Park S, Lee LR, Seo JH, Kang S. Curcumin and tetrahydrocurcumin both prevent osteoarthritis symptoms and decrease the expressions of pro-inflammatory cytokines in estrogen-deficient rats. *Genes Nutr* [Internet]. 2016;11(1):1–13. <http://dx.doi.org/10.1186/s12263-016-0520-4>.
67. Zhang Y, Zeng Y. Curcumin reduces inflammation in knee osteoarthritis rats through blocking TLR4 /MyD88/NF-κB signal pathway. *Drug Dev Res*. 2019;80(3):353–9.
68. Buhrmann C, Mobasheri A, Matis U, Shakibaei M. Curcumin mediated suppression of nuclear factor-κB promotes chondrogenic differentiation of mesenchymal stem cells in a high-density co-culture microenvironment. *Arthritis Res Ther*. 2010;12(4).
69. Aho OM, Finnilä M, Thevenot J, Saarakkala S, Lehenkari P. Subchondral bone histology and grading in osteoarthritis. *PLoS One*. 2017;12(3):1–16.
70. Burr DB, Gallant MA. Bone remodelling in osteoarthritis. *Nat Rev Rheumatol*. 2012;8(11):665–73.
71. Oh S, Kyung TW, Choi HS. Curcumin inhibits osteoclastogenesis by decreasing receptor activator of nuclear factor-κB ligand (RANKL) in bone marrow stromal cells. *Mol Cells*. 2008;26(5):486–9.
72. Chen Z, Xue J, Shen T, Ba G, Yu D, Fu Q. Curcumin alleviates glucocorticoid-induced osteoporosis by protecting osteoblasts from apoptosis in vivo and in vitro. *Clin Exp Pharmacol Physiol*. 2016;43(2):268–76.
73. van der Kraan PM, van den Berg WB. Osteophytes: relevance and biology. *Osteoarthr Cartil*. 2007;15(3):237–44.
74. Van Lent PLEM, Blom AB, Van Der Kraan P, Holthuysen AEM, Vitters E, Van Rooijen N, et al. Crucial Role of Synovial Lining Macrophages in the Promotion of Transforming Growth Factor β-Mediated

Osteophyte Formation. *Arthritis Rheum.* 2004;50(1):103–11.

75. Blom AB, van Lent PLEM, Holthuisen AEM, van der Kraan PM, Roth J, van Rooijen N, et al. Synovial lining macrophages mediate osteophyte formation during experimental osteoarthritis. *Osteoarthr Cartil.* 2004;12(8):627–35.
76. Wang Q, Ye C, Sun S, Li R, Shi X, Wang S, et al. Curcumin attenuates collagen-induced rat arthritis via anti-inflammatory and apoptotic effects. *Int Immunopharmacol.* 2019;72(May 2018):292–300.
77. Bapat S, Hubbard D, Munjal A, Hunter M, Fulzele S. Pros and cons of mouse models for studying osteoarthritis. *Clin Transl Med [Internet].* 2018;7(1). <https://doi.org/10.1186/s40169-018-0215-4>.
78. McCoy AM. Animal Models of Osteoarthritis: Comparisons and Key Considerations. *Vet Pathol.* 2015;52(5):803–18.

Figures

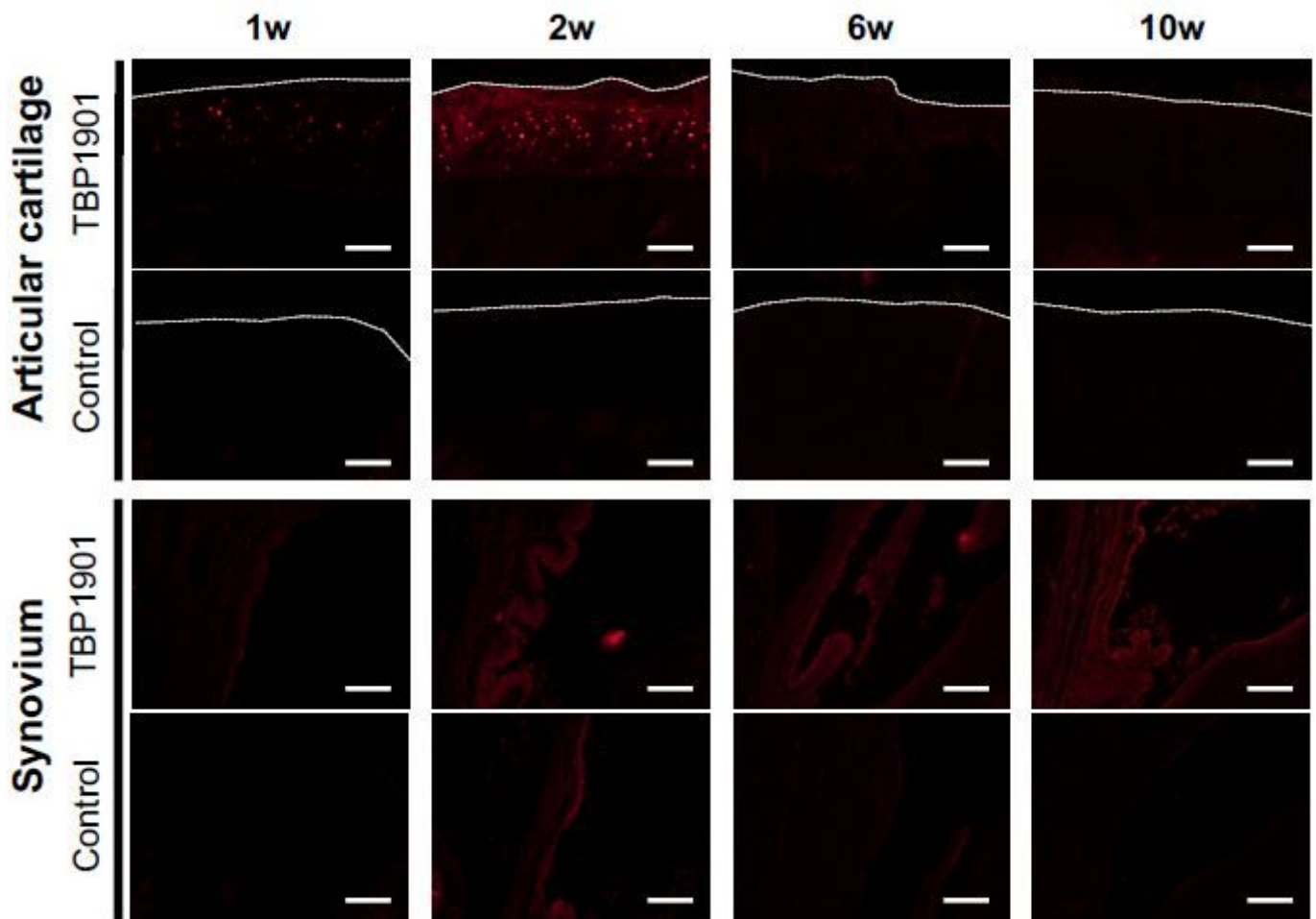


Figure 1

Fluorescence microscopy images of the articular cartilage and synovium of the knee joints. Representative histological images. Curcumin fluorescence (red) was confirmed in the articular cartilage

and synovium at all experimental periods in rats injected with TBP1901. The dotted line indicates the articular cartilage surface line. Magnification: $\times 125$. Scale bar: $100\mu\text{m}$

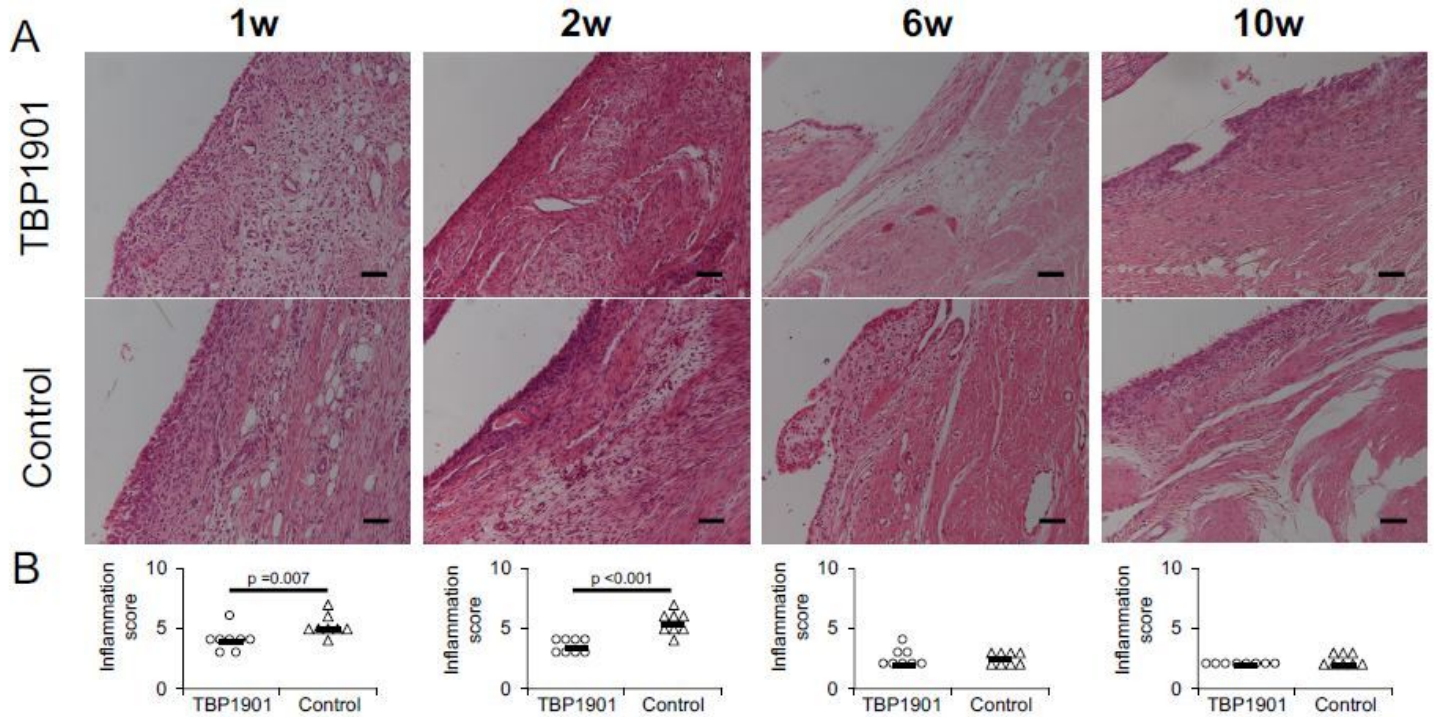


Figure 2

Histological images stained with H/E and synovial inflammation scores in the knee joint. A. Representative histological images of the knee synovium are shown. Magnification: $\times 200$. Scale bar: $100\mu\text{m}$. B. TBP1901 injections in rats with DMM significantly reduced the inflammation scores at 1 and 2 weeks compared with the control group. Values are the medians in the TBP1901 and control groups at several time points ($n=8$, each). P-values were calculated using the Wilcoxon test.

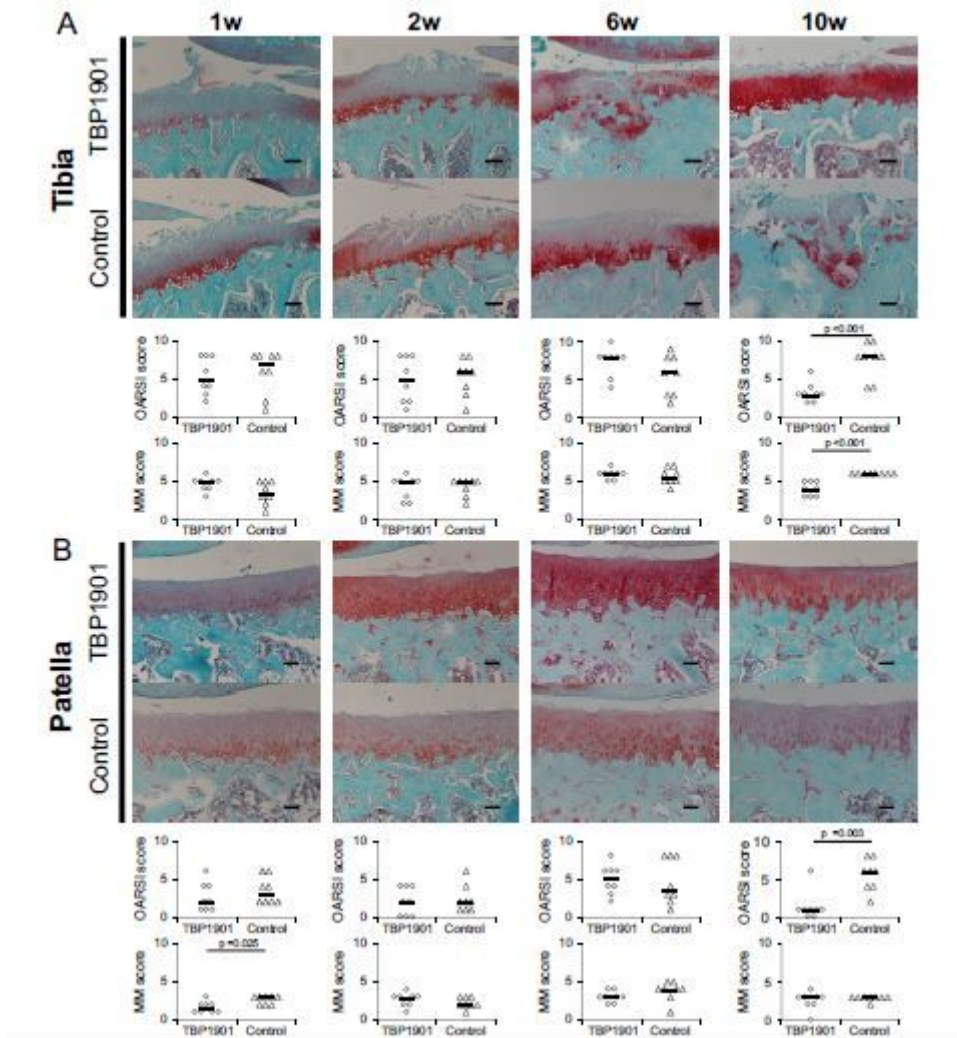


Figure 3

Histological images of SafraninO/Alcian blue stained specimens and OA scores. OA scores were evaluated for the articular cartilage on the tibial plateau in the tibiofemoral joint A. and the patella in patellofemoral joints B. using Osteoarthritis Research Society International (OARSI) scores and Modified Mankin (MM) scores. In the TBP1901 group, the articular cartilage structure ameliorated from 6 to 10 weeks. TBP1901 injections in rats with DMM significantly reduced the OARSI score in the tibia and patella at 10 weeks compared with the control group. TBP1901 injections significantly reduced the MM score in the tibia at 10 weeks and in the patella at 1 week. Values are the medians in the TBP1901 and control groups at several time points (n=8, each). P-values were calculated using the Wilcoxon test. Magnification: $\times 100$. Scale bar: $100\mu\text{m}$

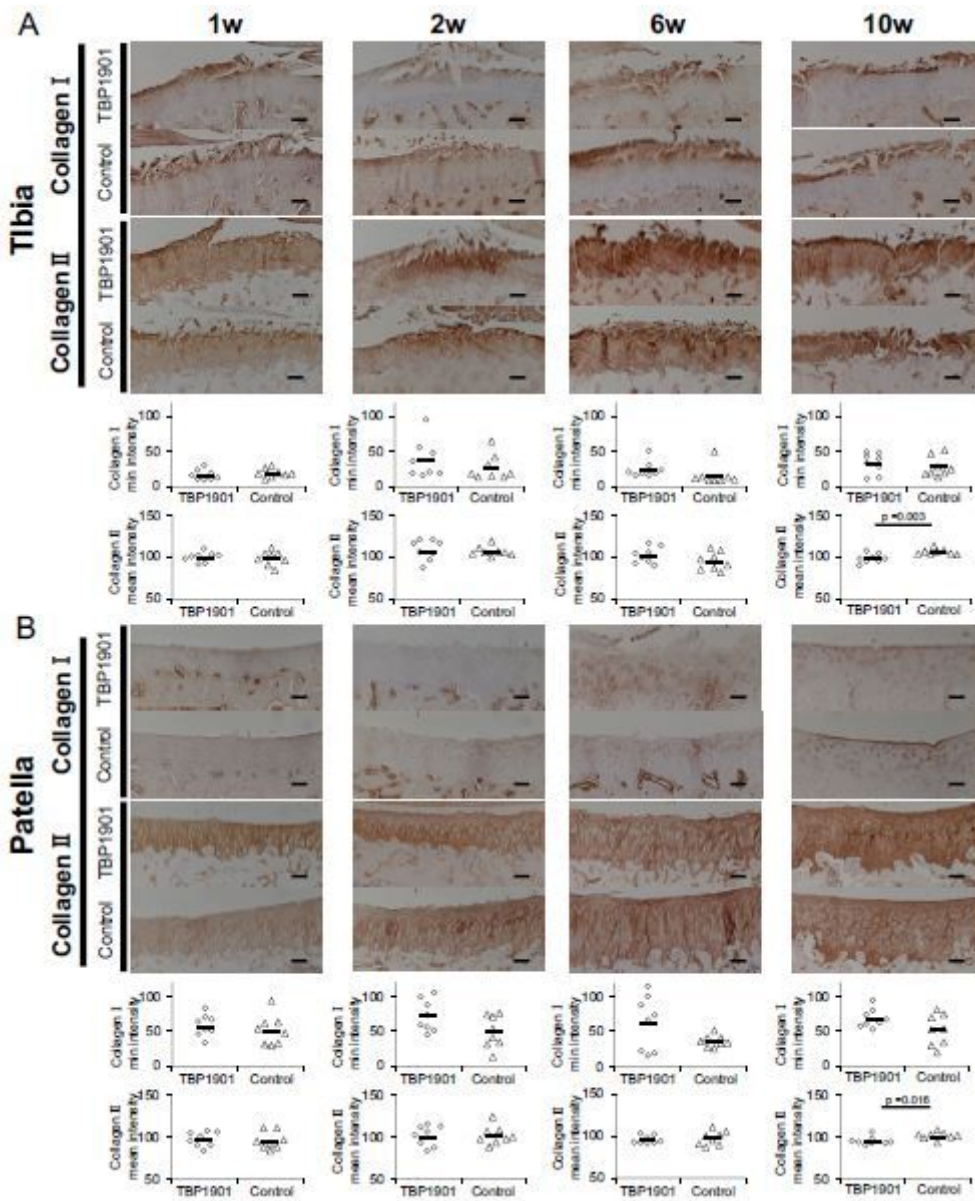


Figure 4

TBP1901 injections increased type II collagen expression in 10 weeks. A. Immunohistochemical images with type I and II collagen and quantitative analyses in the tibia of the tibiofemoral joint. B. Immunohistochemical images with type I and II collagen and quantitative analyses in the patella of the patellofemoral joint. The expression of type I and type II collagen was analyzed by measuring the minimum and mean intensity values using ImageJ, on a scale from 0 (maximum staining) to 255 (no staining). Values are the means in the TBP1901 and control groups at several time points (n=8, each). P-values were calculated using Welch's T-test. Magnification: $\times 100$. Scale bar: $100\mu\text{m}$

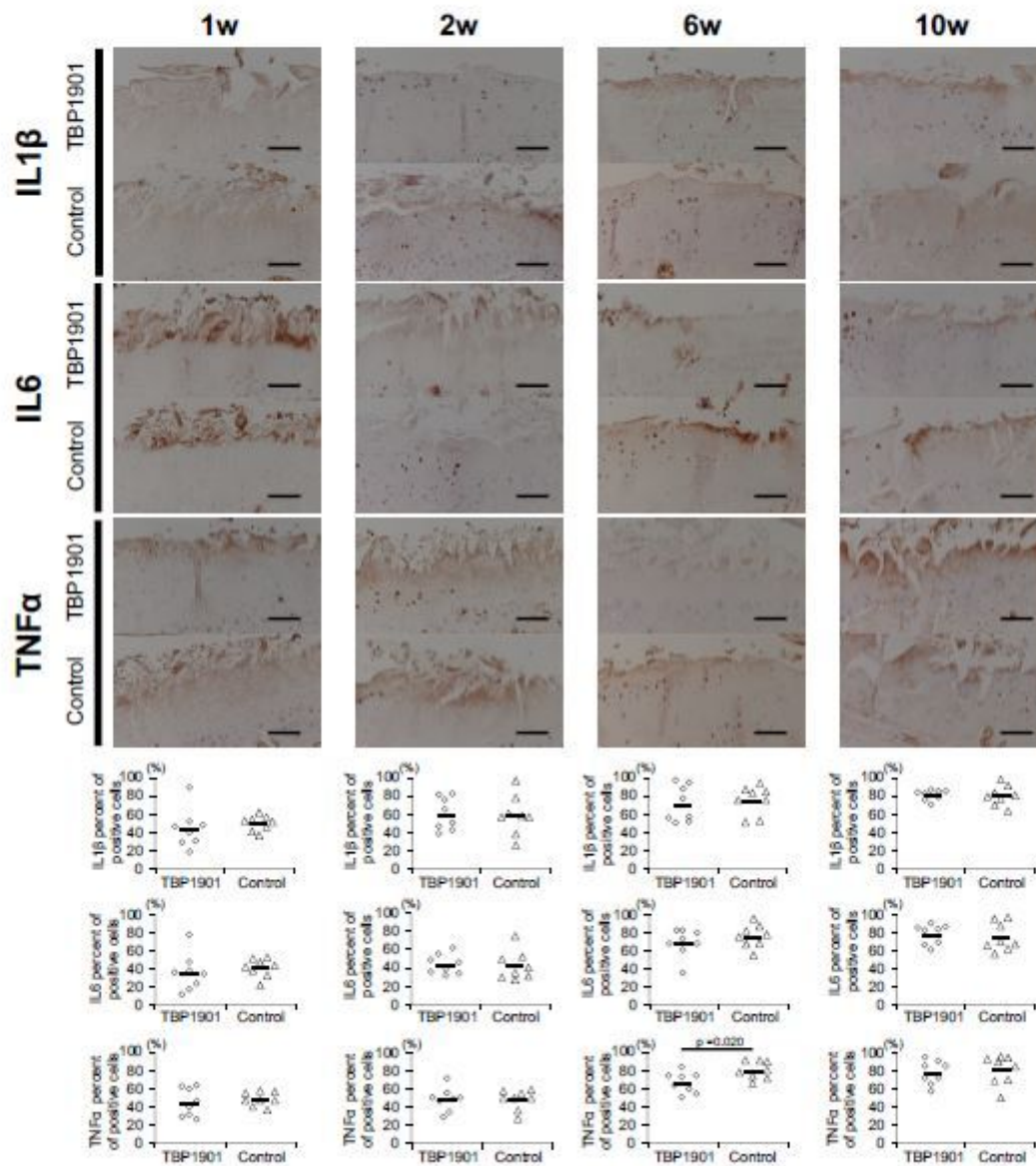


Figure 5

TBP1901 injections suppressed the expression of pro-inflammatory cytokines in the articular cartilage of the tibiofemoral joint. Representative immunohistochemical images of IL1 β , IL6, and TNF α in the articular cartilage of the tibia are shown in the upper row. The percentages of positive cells are shown in the lower row. The percentage of TNF α -positive cells in the TBP1901 group was significantly reduced at 6 weeks compared with the control group. Values are the means in the TBP1901 and control groups at several time points (n=8, each). P-values were calculated using Welch's T-test. Magnification: $\times 200$. Scale bar: 100 μ m

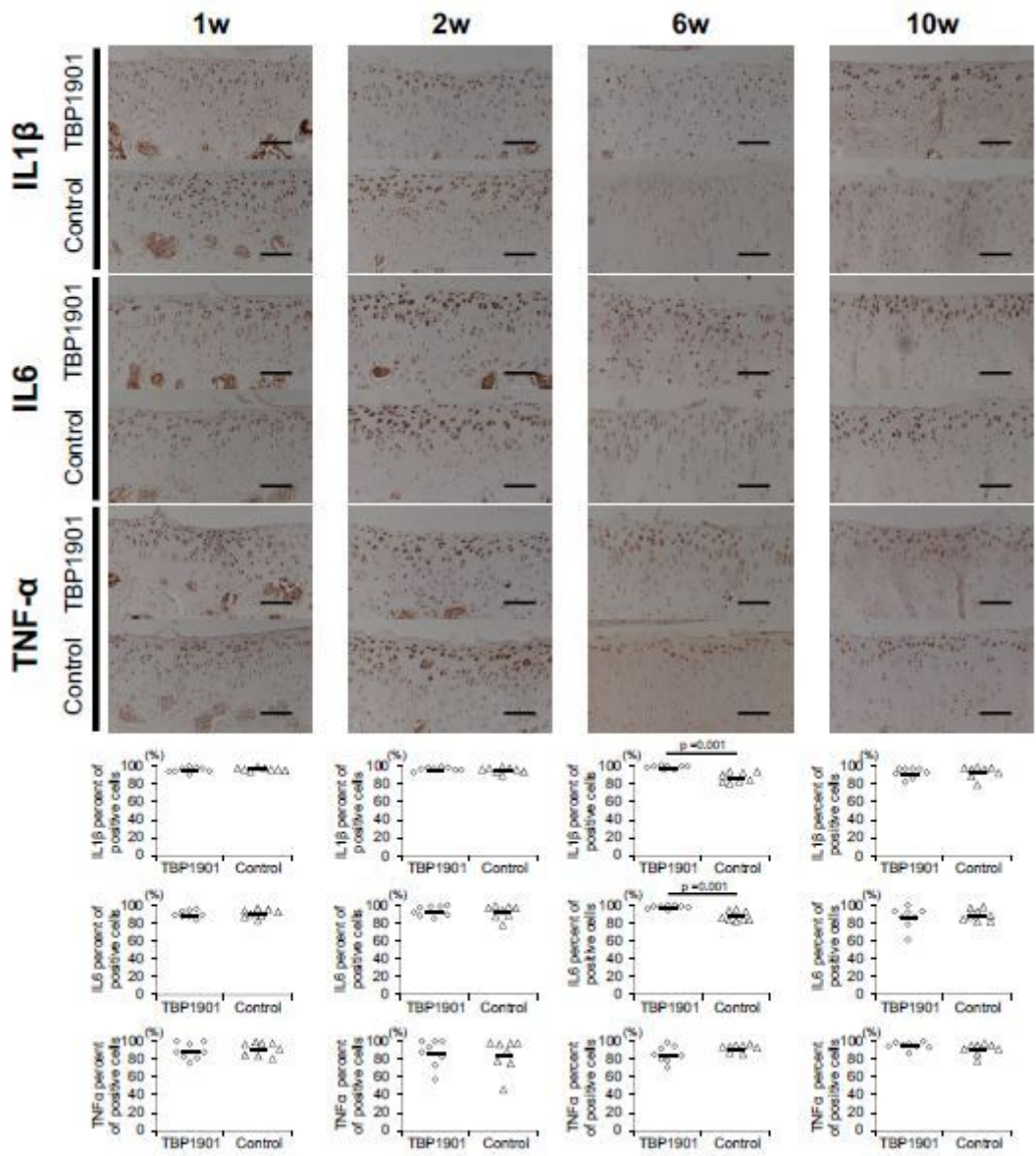


Figure 6

TBP1901 injections did not suppress the expression of pro-inflammatory cytokines in the articular cartilage of the TBP1901 patellofemoral joint. Representative immunohistochemical images of IL1 β , IL6, and TNF α in the articular cartilage of the patella are shown in the upper row. The percentages of positive cells are shown in the lower row. The percentages of IL1 β and IL6 positive cells in the TBP1901 group were significantly higher at 6 weeks compared with the control group. Values are the means in the TBP1901 and control groups at several time points (n=8, each). P-values were calculated using Welch's T-test. Magnification: $\times 200$. Scale bar: 100 μ m

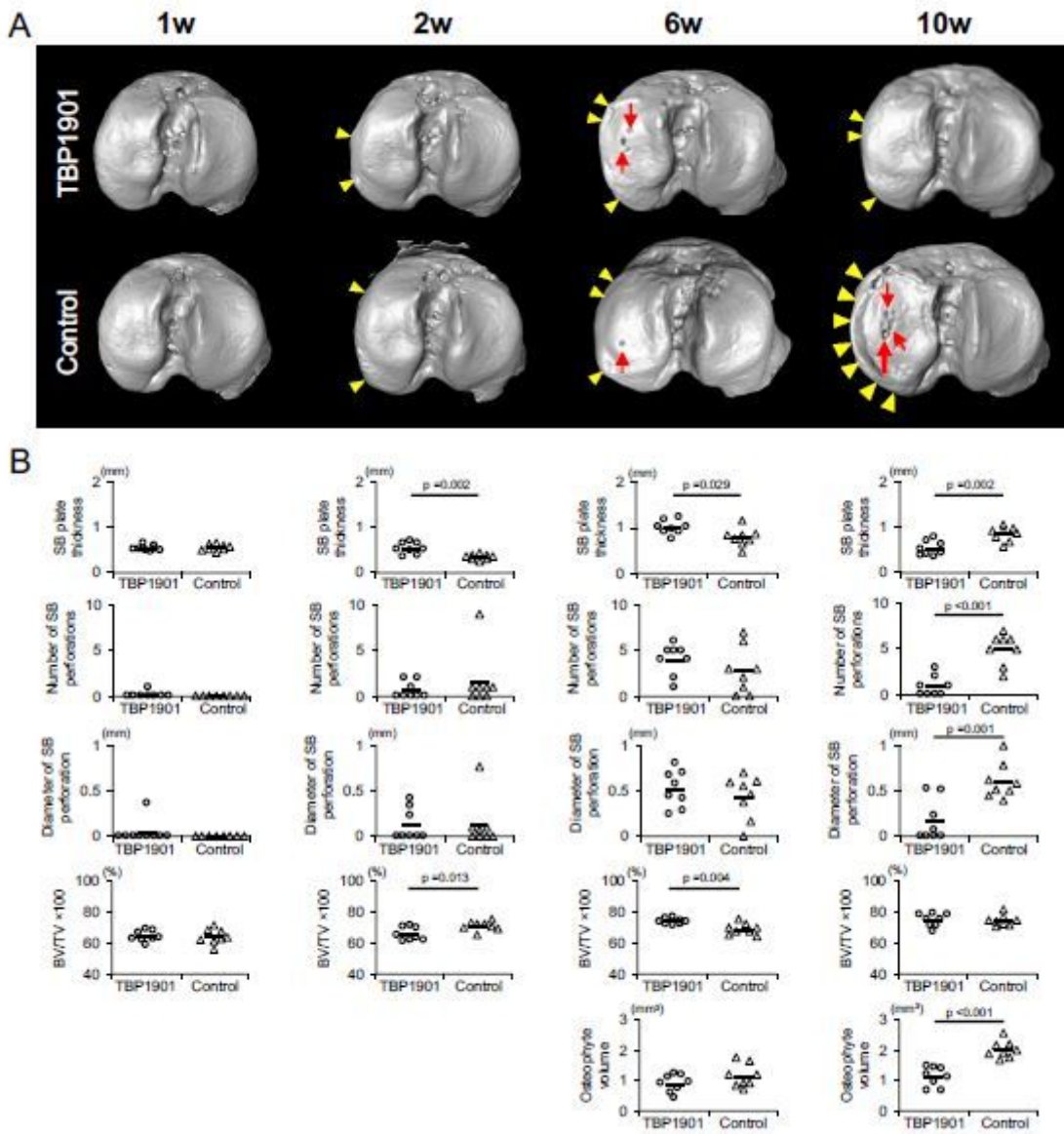


Figure 7

TBP1901 injections prevented excessive bone formation and ameliorated subchondral bone (SB) plate perforations. A. Representative three-dimensional micro-CT images of the SB in the tibial plateau. SB plate perforations (red arrows) were found in the medial tibial plateau, especially at 6 and 10 weeks. Osteophytes (yellow arrowheads) were confirmed on the medial margin at 2, 6, and 10 weeks. B. TBP1901 injections significantly suppressed SB plate thinning in 2 weeks and reduced SB plate thickness, number of SB plate perforations, diameter of SB plate perforations, and osteophyte volume in 10 weeks. Values are the means in all measurements at several time points (n=8, each). P-values were calculated using Welch's T-test for all measurements.

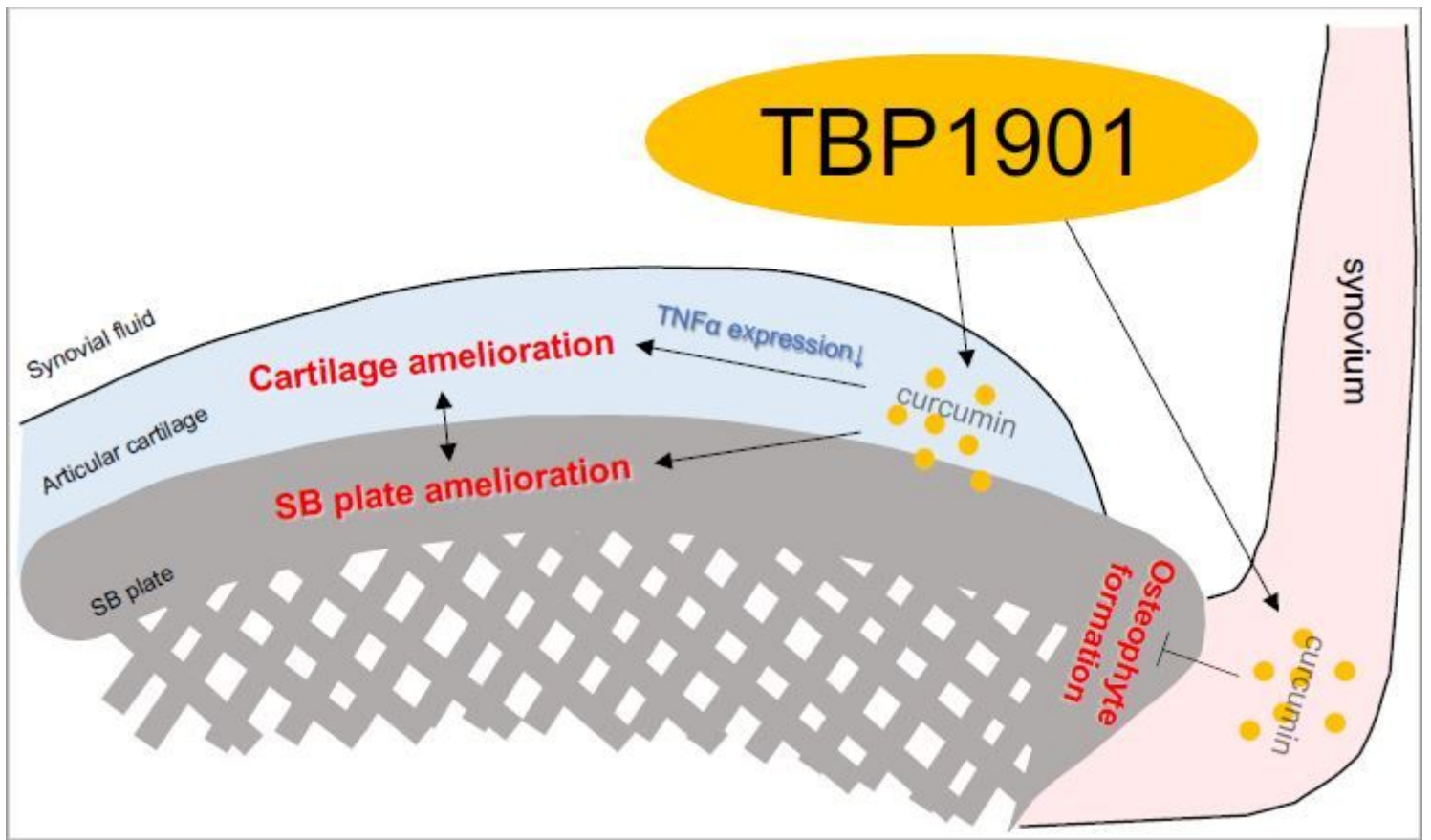


Figure 8

Graphical abstract for the effects of the intra-articular injection of TBP1901 on the amelioration of OA development in the rat OA model (DMM). Curcumin was found in the articular cartilage and synovium after TBP1901 injection. Curcumin suppressed inflammation and osteophyte formation, and ameliorated the articular cartilage and subchondral bone (SB) pathology.

Supplementary Files

This is a list of supplementary files associated with this preprint. Click to download.

- [supptable1.pdf](#)
- [suppfig1BW.pdf](#)